Dynamic Nuclear Structure Emerges from Chromatin Cross-Links and Motors

Kuang Liu, Alison E. Patteson, Edward J. Banigan, and J. M. Schwarz

Phys. Rev. Lett. **126**, 158101 — Published 14 April 2021

DOI: 10.1103/PhysRevLett.126.158101

Dynamic nuclear structure emerges from chromatin crosslinks and motors

Kuang Liu[1], Alison E. Patteson[1], Edward J. Banigan[2], J. M. Schwarz[1,3]
[1] *Department of Physics and BioInspired Syracuse, Syracuse University, Syracuse, NY USA,* [2] *Institute for Medical Engineering and Science and Department of Physics, MIT, Cambridge, MA* [3] *Indian Creek Farm, Ithaca, NY, USA*
(Dated: March 9, 2021)

The cell nucleus houses the chromosomes, which are linked to a soft shell of lamin protein filaments. Experiments indicate that correlated chromosome dynamics and nuclear shape fluctuations arise from motor activity. To identify the physical mechanisms, we develop a model of an active, crosslinked Rouse chain bound to a polymeric shell. System-sized correlated motions occur but require both motor activity *and* crosslinks. Contractile motors, in particular, enhance chromosome dynamics by driving anomalous density fluctuations. Nuclear shape fluctuations depend on motor strength, crosslinking, and chromosome-lamina binding. Therefore, complex chromosome dynamics and nuclear shape emerge from a minimal, active chromosome-lamina system.

The cell nucleus houses the genome, the material containing instructions for building the proteins that a cell needs to function. This material is ~ 1 meter of DNA with proteins, forming chromatin, and it is packaged across multiple spatial scales to fit inside a ~ 10 μm nucleus [1]. Chromatin is highly dynamic; for instance, correlated motion of micron-scale genomic regions over timescales of tens of seconds has been observed in mammalian cell nuclei [2–6]. This correlated motion diminishes both in the absence of ATP and by inhibition of the transcription motor RNA polymerase II, suggesting that motor activity plays a key role [2, 3]. These dynamics occur within the confinement of the cell nucleus, which is enclosed by a double membrane and 10-30-nm thick filamentous layer of lamin intermediate filaments, the lamina [7–9]. Chromatin and the lamina interact through various proteins [10–12] and form structures such as lamina-associated domains (LADs) [13, 14]. Given the complex spatiotemporal properties of a cell nucleus, how do correlated chromatin dynamics emerge and what is their interplay with nuclear shape?

Numerical studies suggest several explanations for correlated chromatin motions. Individual unconfined active semiflexible polymer chains with exponentially correlated noise exhibit enhanced displacement correlations [15]. With confinement, a Rouse chain with long-range hydrodynamic interactions that is driven by extensile dipolar motors can exhibit correlated motion over long length and timescales [4]. Correlations arise due to the emergence of local nematic ordering within the confined globule. However, such local nematic ordering has yet to be observed. In the absence of activity, a confined heteropolymer may exhibit correlated motion, with anomalous diffusion of small loci [16, 17]. However, in marked contrast with experimental results [2, 3], introducing activity in such a model does not alter the correlation length at short timescales and decreases it at longer timescales.

Through interactions or linkages with the lamina, chromatin dynamics may influence the shape of the nuclear lamina. Experiments have begun to investigate this notion by measuring nuclear shape fluctuations [18–20]. Depletion of ATP, the fuel for many molecular motors, diminishes the magnitude of the shape fluctuations, as does the inhibition of RNA polymerase II transcription activity by α-amanitin [20]. Other studies have found that depleting linkages between chromatin and the nuclear lamina results in more deformable nuclei [21, 22], enhanced curvature fluctuations [23], and/or abnormal nuclear shapes [24]. Interestingly, depletion of lamin A in several human cell lines leads to increased diffusion of chromatin, suggesting that chromatin dynamics is also affected by linkages to the lamina [25]. Together, these experiments demonstrate the critical role of chromatin and its interplay with the nuclear lamina in determining nuclear structure.

To understand these results mechanistically, we construct a chromatin-lamina system with the chromatin modeled as an *active* Rouse chain and the lamina as an elastic, polymeric shell with linkages between the chain and the shell. Unlike previous chain and shell models [23, 26, 27], our model has motor activity. We implement a generic and simple type of motor, namely extensile and contractile monopoles, representative of the scalar events considered in a two-fluid model of chromatin [28]. We also include chromatin crosslinks, which may be a consequence of motors forming droplets [29] and/or complexes [30], as well as chromatin binding by proteins, such as heterochromatin protein I (HP1) [31, 32]. Recent rheological measurements of the nucleus support the notion of chromatin crosslinks [26, 27, 32], as does indirect evidence from chromosome conformation capture (Hi-C) [33]. In addition, we explore how the nuclear shape and chromatin dynamics mutually affect each other by comparing results for an elastic, polymeric shell with those of a stiff, undeformable one.

Model: Interphase chromatin is modeled as a Rouse chain consisting of 5000 monomers (each representing $\lesssim 1$ Mb of chromatin) with radius r_c connected by Hookean springs with spring constant K. We include excluded volume interactions with a repulsive, soft-core potential between any two monomers, ij, and a distance, $|\vec{r}_{ij}|$, between their centers, through the potential $U_{ex} = \frac{1}{2}K_{ex}(|\vec{r}_{ij}| - \sigma_{ij})^2$ for $|\vec{r}_{ij}| < \sigma_{ij}$, where

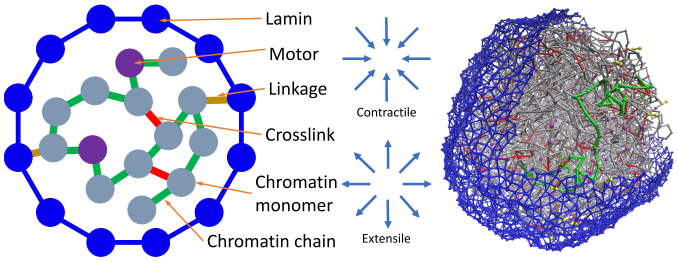

FIG. 1. Left: Two-dimensional schematic of the model. Center: Schematic of the two types of motors. Right: Simulation snapshot. The chromatin polymer is composed of linearly connected monomers, shown in gray. Active chromatin subunits are shown in purple. The lamina is composed of lamin subunits, shown in blue.

$\sigma_{ij} = r_{c_i} + r_{c_j}$, and zero otherwise. Previous mechanical experiments and modeling suggest extensive crosslinking [26, 27, 32], so we include $N_C \leq 2500$ crosslinks between chromatin monomers by introducing a spring between different parts of the chain with the same spring constant as along the chain.

In addition to (passive) thermal fluctuations, we also allow for explicit motor activity along the chain. In simulations with motors, we assign $N_m = 400$ chain monomers to be active. An active monomer has motor strength M and exerts sub-pN force $\mathbf{F_a} = \pm M\hat{r}_{ij}$ on monomers within a fixed range. Active monomers do not experience a reciprocal force, $-\mathbf{F_a}$, so the system is out of equilibrium (see SM, which includes Refs. [34–41]). Motor forces may be attractive or "contractile," drawing in chain monomers, or alternatively, repulsive or "extensile," pushing them away (Fig. 1), similar to other explicit models of motor activity [4, 28, 42]. Since motors *in vivo* are dynamic, unbinding or turning off after some characteristic time, we include a turnover timescale, τ_m, for the motor monomers, after which a motor moves to another position on the chromatin. We study $\tau_m = 20$, corresponding to ~ 10 s, *i.e.*, comparable to the timescale of experimentally observed chromatin motions [2, 3], but shorter than the turnover time RNA polymerase [43].

The lamina is modeled as a layer of 5000 identical monomers connected by springs with the same radii and spring constants as the chain monomers and an average coordination number $z \approx 4.5$, as supported by previous modeling [23, 26, 27] and imaging experiments [7–9]. Shell monomers also have a repulsive soft core. We model the chromatin-lamina linkages as N_L permanent springs with stiffness K between shell monomers and chain monomers (Fig. 1).

The system evolves via Brownian dynamics, obeying the overdamped equation of motion: $\xi\dot{\mathbf{r}}_i = (\mathbf{F_{br}} + \mathbf{F_{sp}} + \mathbf{F_{ex}} + \mathbf{F_a})$, where $\mathbf{F_{br}}$ denotes the (Brownian) thermal force, $\mathbf{F_{sp}}$ denotes the harmonic forces due to chain springs, chromatin crosslink springs, and chromatin-lamina linkage springs, and $\mathbf{F_{ex}}$ denotes the force due to excluded volume. We use Euler updating, a time step of $d\tau = 10^{-4}$, and a total simulation time of $\tau = 500$. For the passive system, $\mathbf{F_a} = 0$. In addition to the deformable shell, we also simulate a hard shell by freezing out the motion of the shell monomers. To assess the structural properties in steady state, we measure both the radial globule, R_g, of the chain and the self-contact probability. After these measures do not appreciably change with time, we consider the system to be in steady state. See SM for these measurements, simulation parameters, and other simulation details.

Results: We first look for correlated chromatin motion in both hard shell and deformable shell systems. We do so by quantifying the correlations between the displacement fields at two different points in time. Specifically, we compute the normalized spatial autocorrelation function defined as $C_r(\Delta r, \Delta\tau) = \frac{1}{N(\Delta r)} \sum_{N(\Delta r)} \frac{<\mathbf{d_i}(\mathbf{r},\mathbf{\Delta}\tau)\cdot\mathbf{d_j}(\mathbf{r}+\mathbf{\Delta r},\mathbf{\Delta}\tau)>}{<\mathbf{d^2}(\mathbf{r},\mathbf{\Delta}\tau)>}$, where $\Delta\tau$ is the time window, Δr is the distance between the centers of the two chain monomers at the beginning of the time window, $N(\Delta r)$ is the number of ij pairs of monomers within distance Δr of each other at the beginning of the time window, and $\mathbf{d_i}$ is the displacement of the i^{th} chain monomer during the time window, defined with respect to the origin of the system. Two chain monomers moving in the same direction are positively correlated, while monomers moving in opposite directions are negatively correlated.

Fig. 2 shows $C_r(\Delta r, \Delta\tau)$ for passive and active samples in both hard shell (Figs. 2 (a) and (b)) and soft shell cases for $N_C = 2500$, $N_L = 50$, $M = 5$, and $\tau_m = 20$ (Figs. 2 (e) and (f)) (see SM for results with other parameters). Both the passive and active samples exhibit short-range correlated motion when the time window is small, *i.e.*, $\Delta\tau < 5$. However, for longer time windows, both the extensile and contractile active samples exhibit more long-range correlated motion than the passive case. Correlations are also stronger for longer τ_m (see SM), similar to findings for individual active polymers [15]. These correlations are visible in quasi-2d spatial maps of instantaneous chromatin velocities, which show large regions of coordinated motion in the active, soft shell case (Figs. 2 (c) and (g)).

To extract a correlation length to study the correlations as a function of both N_C and N_L, we use a Whittel-Marten (WM) model fitting function, $C_r(r) = \frac{2^{1-\nu}}{\Gamma(\nu)} \left(\frac{r}{r_{cl}}\right)^{\nu} K_\nu \left(\frac{r}{r_{cl}}\right)$, for each time window (Fig. 2 (f)) [3]. The parameter ν is approximately 0.2 for all cases studied. For the hard shell, the correlation length decreases with number of linkages (Fig. 2 (d)). This trend is opposite in deformable shell case with activity and long time lags (Fig. 2 (h)). For the hard shell, linkages effectively break up the chain into uncorrelated regions. For the soft shell, the shell deforms in response to active fluctuations in the chain. For both types of shells, the correlation length increases with the number of crosslinks (Figs. 2 (d) and (h)), with a more significant increase in the soft shell active case. It is also interesting to note

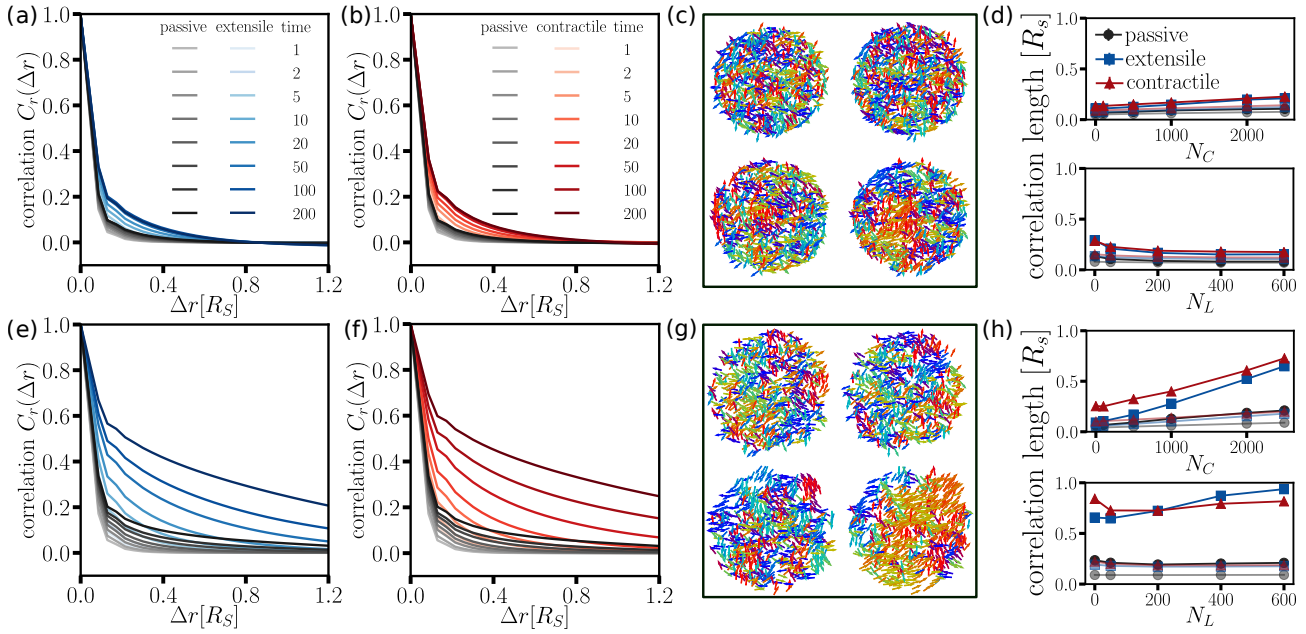

FIG. 2. (a) The spatial autocorrelation function $C_r(\Delta r, \Delta\tau)$ for passive and extensile cases at different time lags, $\Delta\tau$, for the hard shell, while (b) shows the contractile and passive case. (c) Two-dimensional vector fields for $\Delta\tau = 5$ (left), 50 (right) for the passive case (top) and the contractile case (bottom). (d) The correlation length as a function of N_L and N_C for the two time lags in (c). (e∼h): The bottom row shows the same as the top row, but with a soft shell. Lengths shown in units of the hard-shell radius, $R_s = 10$. See SM for representative fits to obtain the correlation length.

that the lengthscale for the contractile case is typically larger than that of the extensile case, at least for smaller numbers of linkages.

Given the differences in correlation lengths between the hard and soft shell systems, we looked for enhanced motion of the system in the soft shell case. Enhanced motion has been predicted for active polymers [15, 44, 45] and observed in active particle systems confined by a deformable shell [46]. Similarly, we observe the active chain system moving faster than diffusively (see SM). In the shell's center-of-mass frame, the correlation length is decreased, but still larger than in the hard shell simulations (see SM). Interestingly, experiments demonstrating large-scale correlated motion measure chromatin motion with an Eulerian specification (*e.g.*, by particle image velocimetry) and do not subtract off the global center of mass [2, 3, 6]. However, one experiment noted that they observed drift of the nucleus on a frame-to-frame basis, but considered it negligible over the relevant time scales [3]. Additionally, global rotations, which we have not considered, could yield large-scale correlations.

We also study the mean-squared displacement of the chromatin chain to determine if the experimental feature of anomalous diffusion is present. Figs. 3 (a) and (c) show the mean-squared displacement of the chain with $N_L = 50$ and $N_C = 2500$ as measured with reference to the center-of-mass of the shell for both the hard shell and soft shell cases, respectively. For the hard shell, the passive chain initially moves subdiffusively with an exponent of $\alpha \approx 0.5$, which is consistent with an uncrosslinked Rouse chain with excluded volume interactions [47]. However, the passive system crosses over to potentially glassy behavior after a few tens of simulation time units. We present $N_C = 0$ case in the inset to Fig. 3 (a) for comparison to demonstrate that crosslinks

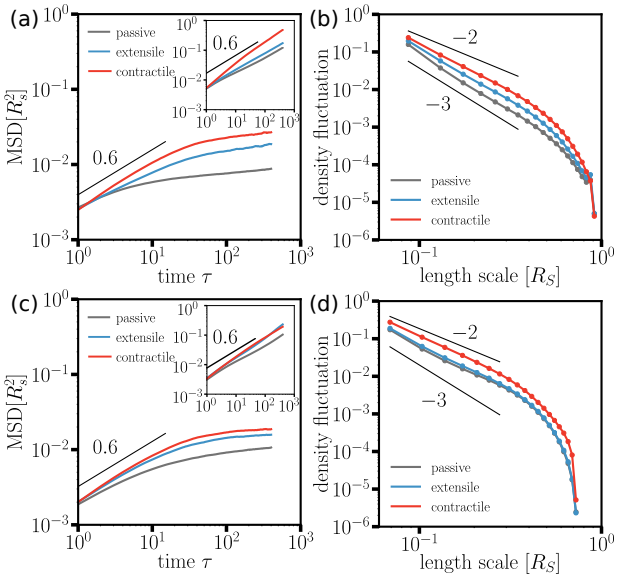

FIG. 3. (a) MSD for the hard shell case with $N_C = 2500$, $N_L = 50$, and $M = 5$. For the inset, $N_C = 0$. (b) Density fluctuations for the same parameters as in (a). Figures (c) and (d) show the soft shell equivalent to (a) and (b).

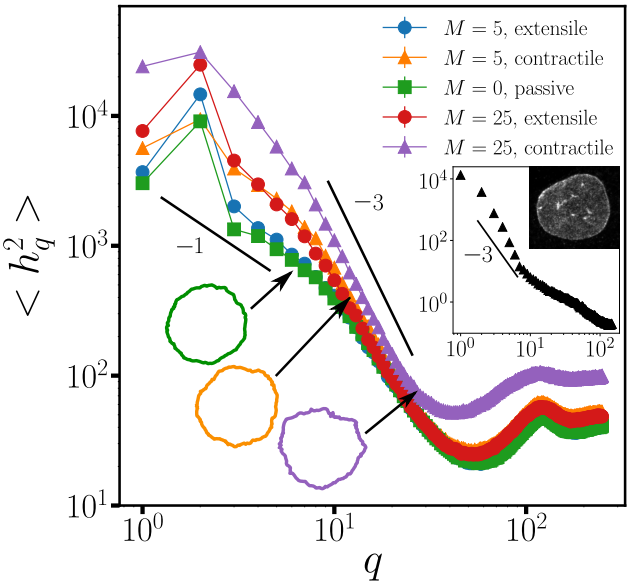

FIG. 4. Power spectrum of the shape fluctuations with $N_L = 50$ and $N_C = 2500$ for the passive and both active cases. Different motor strengths are shown. The inset shows experimental data from mouse embryonic fibroblasts with an image of a nucleus with lamin A/C stained.

potentially drive a gel-sol transition, as observed in prior experiments [48]. The active hard shell samples exhibit larger displacements than passive samples, with $\alpha \sim 0.6$ initially before crossing over to a smaller exponent at longer times.

Additionally, the contractile system exhibits larger displacements than the extensile system. We found that a broader spectrum of steady-state density fluctuations for the contractile system drive this behavior (Fig. 3 (b)). This generates regions of lower density into which the chain can move, leading to increased motility. The active cases exhibit anomalous density fluctuations, with the variance in the density falling off more slowly than inverse length cubed (in 3D). Finally, the MSD in the hard shell case is suppressed by more boundary linkages or crosslinks (see SM). For the soft shell case, we observe similar trends as the hard shell.

Next, we examine nuclear shape. In Fig. 4, we plot the power spectrum of the shape fluctuations of the shell for a central cross-section as a function of wavenumber q for different motor strengths. Shape fluctuations are less significant for both the passive and extensile systems than for the contractile systems. This difference could be due to more anomalous density fluctuations in the contractile case, demonstrating that chromatin spatiotemporal dynamics directly impacts nuclear shape. The fluctuation spectrum is dominated by an approximate q^{-3} decay, which is characteristic of bending-dominated fluctuations in a cross-section of a fluctuating shell [49–53]. Bending fluctuations are consistent with previous experimental observations [20] and simulations [26] of cell nuclei, theoretical predictions for membranes embedded with active particles [54, 55], and our experiments measuring nuclear shape fluctuations in mouse embryonic fibroblasts (MEFs) (inset to Fig. 4 and see SM for materials and methods). For the passive case, we also observe a narrow regime of approximate q^{-1} scaling at small q, which is characteristic of membrane tension, and saturation at large q due to the discretization of the system. For the active cases, we only clearly observe the latter trend. Additionally, the amplitude of the shape fluctuations increases with motor strength, N_C, and N_L (see SM).

Discussion: We have studied a composite chromatin-lamina system in the presence of activity, crosslinking, and linkages between chromatin and the lamina. Our model captures correlated chromatin motion on the scale of the nucleus in the presence of both activity and crosslinks (Fig. 2). The deformability of the shell also plays a role. We find that global translations of the composite soft shell system contribute to the correlations. We observe anomalous diffusion for the chromatin (Figs. 3 (a) and (c)), as has been observed experimentally [25], with a crossover to a smaller anomalous exponent driven by the crosslinking [48]. Interestingly, the contractile system exhibits a larger MSD than the extensile one, which is potentially related to the more anomalous density fluctuations in the contractile case (Figs. 3 (b) and (d)). Finally, nuclear shape fluctuations depend on motor strength and on amounts of crosslinking and chromatin-lamina linkages (Fig. 4). Notably, the contractile case exhibits more dramatic changes in the shape fluctuations as a function of wavenumber as compared to the extensile case.

Our short-range, overdamped model contrasts with an earlier confined, active Rouse chain interacting with a solvent via long-range hydrodynamics [4]. While both models generate correlated chromatin dynamics, with the earlier model, such correlations are generated only with extensile motors that drive local nematic ordering of the chromatin chain [4]. Moreover, correlation lengths in our model are significantly larger than those obtained in a previous confined active, heteropolymer simulation [16]. Activity in this earlier model is modeled as extra-strong thermal noise such that the correlation length decreases at longer time windows as compared to the passive case. This decrease contrasts with our results (Figs. 2 (d) and (h)) and experiments [3]. In addition, our model takes into account deformability of the shell and the chromatin-lamina linkages. Future experiments could potentially distinguish these mechanisms by looking for prominent features of our model, such as a dependence on chromatin bridging proteins and linkages to the lamina and effects of whole-nucleus motions.

Further spatiotemporal studies of nuclear shape could investigate the role of the cytoskeleton. Particularly interesting would be *in vivo* studies with vimentin-null cells, which have minimal mechanical coupling between the cytoskeleton and the nucleus. Vimentin is a cytoskeletal intermediate filament that forms a protective

cage on the outside of the nucleus and helps regulate the nucleus-cytoplasm coupling and, thus, affects nuclear shape [56]. The amplitudes of the nuclear shape fluctuations in vimentin-null cells may increase due to a softer perinuclear shell; alternatively, they may decrease due to fewer linkages between the nucleus and the mechanically active cytoskeleton, which may impact nuclear shape fluctuations [18, 19, 57].

There are intriguing parallels between cell shape [58–60] and nuclear shape with cell shape being driven by an underlying cytoskeletal network—an active, filamentous system driven by polymerization/depolymerization, crosslinking, and motors, both individually and in clusters, that can remodel, bundle and even crosslink filaments. Given the emerging picture of chromatin motors acting collectively [29, 30], just as myosin motors do [61], the parallels are strengthened. Moreover, the more anomalous density fluctuations for the contractile motors as compared to the extensile motors could potentially be relevant in random actin-myosin systems typically exhibiting contractile behavior, even though either is allowed by a statistical symmetry [62]. On the other hand, distinct physical mechanisms may govern nuclear shape since the chromatin fiber is generally more flexible than cytoskeletal filaments and the lamina is stiffer than the cell membrane.

We now have a minimal chromatin-lamina model that can be augmented with additional factors, such as different types of motors—dipolar, quadrupolar, and even chiral, such as torque dipoles. Chiral motors may readily condense chromatin just as twirling a fork "condenses" spaghetti. Finally, there is now compelling evidence that nuclear actin exists in the cell nucleus [63], but its form and function are under investigation. Following reports that nuclear actin filaments may alter chromatin dynamics and nuclear shape [64–66], we propose that short, but stiff, actin filaments acting as stir bars could potentially increase the correlation length of micron-scale chromatin dynamics, while chromatin motors such as RNA polymerase II drive the dynamics. Including such factors will help us further quantify nuclear dynamics to determine, for example, mechanisms for extreme nuclear shape deformations, such as nuclear blebs [67, 68], and ultimately how nuclear spatiotemporal structure affects nuclear function.

EJB thanks Andrew Stephens for helpful discussions and critically reading the manuscript. JMS acknowledges financial support from NSF-DMR-1832002 and from the DoD via an Isaac Newton Award. JMS and AEP acknowledge financial support from a CUSE grant. EJB was supported by the NIH Center for 3D Structure and Physics of the Genome of the 4DN Consortium (U54DK107980), the NIH Physical Sciences-Oncology Center (U54CA193419), and NIH grant GM114190.

[1] J. H. Gibcus and J. Dekker, Mol. Cell **49**, 773 (2013).
[2] A. Zidovska, D. Weitz, and T. Mitchison, Proc. Natl. Acad. Sci. U. S. A. **110**, 15555 (2013).
[3] H. A. Shaban, R. Barth, and K. Bystricky, Nucleic Acids Res. **46**, 11202 (2018).
[4] D. Saintillan, M. J. Shelley, and A. Zidovska, Proc. Natl. Acad. Sci. U. S. A. **115**, 11442 (2018).
[5] R. Barth, K. Bystricky, and H. A. Shaban, Sci. Adv. **6**, eaaz2196 (2020).
[6] H. A. Shaban, R. Barth, L. Recoules, and K. Bystricky, Genome Biol. **21**, 1 (2020).
[7] T. Shimi, M. Kittisopikul, J. Tran, A. E. Goldman, S. A. Adam, Y. Zheng, K. Jaqaman, and R. D. Goldman, Mol. Biol. Cell **26**, 4075 (2015).
[8] J. Mahamid and et al., Science **351**, 969 (2016).
[9] Y. Turgay and et al., Nature **543**, 261 (2017).
[10] T. Dechat and et al., Genes Dev. **22**, 832 (2008).
[11] I. Solovei and et al., Cell **152**, 584 (2013).
[12] R. de Leeuw, Y. Gruenbaum, and O. Medalia, Trends Cell Biol. **28**, 34 (2018).
[13] L. Guelen and et al., Nature **453**, 948 (2008).
[14] B. van Steensel and A. S. Belmont, Cell **169**, 780 (2017).
[15] A. Ghosh and N. S. Gov, Biophys. J. **107**, 1065 (2014).
[16] L. Liu, G. Shi, D. Thirumalai, and C. Hyeon, PLoS Comp. Biol. **14**, e1006617 (2018).
[17] M. DiPierro, D. A. Potoyan, P. G. Wolynes, and J. N. Onuchic, Proc. Natl. Acad. Sci. U. S. A. **115**, 7753 (2018).
[18] S. Talwar, A. Kumar, M. Rao, G. I. Menon, and G. V. Shivashankar, Biophys. J. **104**, 553 (2013).
[19] E. Makhija, D. S. Jokhun, and G. V. Shivashankar, Proc. Natl. Acad. Sci. **113**, E32 (2016).
[20] F. Y. Chu, S. C. Haley, and A. Zidovska, Proc. Natl. Acad. Sci. U. S. A. **114**, 10338 (2017).
[21] C. Guilluy and et al., Nat. Cell Biol. **16**, 376 (2014).
[22] S. M. Schreiner, P. K. Koo, Y. Zhao, S. G. J. Mochrie, and M. C. King, Nat. Comm. **6**, 7159 (2015).
[23] M. C. Lionetti, S. Bonfanti, M. Fumagalli, Z. Budrikis, F. Font-Clos, G. Costantini, O. Chepizhko, S. Zapperi, and C. La Porta, Biophys. J. **118**, 3219 (2020).
[24] A. D. Stephens, E. J. Banigan, and J. F. Marko, Curr. Opin. Cell Biol. **58**, 76 (2019).
[25] I. Bronshtein and et al., Nat. Comm. **6**, 8044 (2015).
[26] E. J. Banigan, A. D. Stephens, and J. F. Marko, Biophys. J. **113**, 1654 (2017).
[27] A. D. Stephens, E. J. Banigan, S. A. Adam, R. D. Goldman, and J. F. Marko, Mol. Biol. Cell **28**, 1984 (2017).
[28] R. Bruinsma, A. Y. Grosberg, Y. Rabin, and A. Zidovska, Biophys. J. **106**, 1871 (2014).
[29] I. I. Cisse and et al., Science **341**, 664 (2013).
[30] R. Nagashima and et al., J. Cell Biol. **218**, 1511 (2019).
[31] F. Erdel and et al., Cell **78**, 236 (2020).
[32] A. R. Strom, R. J. Biggs, E. J. Banigan, X. Wang, K. Chiu, C. Herman, J. Collado, F. Yue, J. C. Ritland Politz, L. J. Tait, D. Scalzo, A. Telling, M. Groudine, C. P. Brangwynne, J. F. Marko, and A. D. Stephens, bioRxiv:2020.10.09.331900 (2020).
[33] H. Belaghzal and et al., biorXiv:704957 (2019).
[34] H. D. Ou, S. Phan, T. J. Deerinck, A. Thor, M. H. Ellisman, and C. C. O'Shea, Science **357**, (6349):eaag0025 (2017).

[35] M. Falk, Y. Feodorova, N. Naumova, M. Imakaev, B. R. Lajoie, H. Leonhardt, B. Joffe, J. Dekker, G. Fudenberg, I. Solovei, and L. A. Mirny, Nature **570**, 395 (2019).

[36] H. Kang, Y.-G. Yoon, D. Thirumalai, and C. Hyeon, Phys. Rev. Lett. **115**, 198102 (2015).

[37] E. J. Banigan and L. A. Mirny, Current Opinion in Cell Biology **64**, 124 (2020).

[38] D. Gerlich, B. Koch, F. Dupeux, J. M. Peters, and J. Ellenberg, Curr. Biol. **16**, 1571 (2006).

[39] E. Lieberman-Aiden, N. van Berkum, L. Williams, M. Imakaev, T. Ragoczy, A. Telling, I. Amit, B. R. Lajoie, P. J. Sabo, M. O. Dorschner, R. Sandstrom, B. Bernstein, M. A. Bender, M. Groudine, A. Gnirke, J. Stamatoyannopoulos, L. A. Mirny, E. S. Lander, and J. Dekker, Science **326**, 289 (2009).

[40] J. Dekker and L. Mirny, Cell **164**, 1110 (2016).

[41] L. D. Landau, L. P. Pitaevskii, A. M. Kosevich, and E. M. Lifshitz, *Theory of Elasticity*, 3rd ed. (Butterworth-Heinemann, 2012).

[42] R. K. Manna and P. B. S. Kumar, Soft Matter **15**, 477 (2019).

[43] X. Darzacq, Y. Shav-Tal, V. De Turris, Y. Brody, S. M. Shenoy, R. D. Phair, and R. H. Singer, Nature structural & molecular biology **14**, 796 (2007).

[44] D. Osmanović and Y. Rabin, Soft Matter **13**, 963 (2017).

[45] S. Chaki and R. Chakrabarti, J. Chem. Phys. **150**, 094902 (2019).

[46] M. Paoluzzi, D. L. R., M. C. Marchetti, and L. Angelini, Sci. Reps. **6**, 34146 (2016).

[47] M. Rubinstein and R. H. Colby, *Polymer Physics* (Oxford University Press, New York, 2003).

[48] N. Khanna, Y. Zhang, J. S. Lucas, O. K. Dudko, and C. Murre, Nat. Comm. **10**, 2771 (2019).

[49] S. T. Milner and S. A. Safran, Phys. Rev. A **36**, 4371 (1987).

[50] J. F. Faucon, M. D. Mitov, P. Méléard, I. Bivas, and P. Bothorel, Journal de Physique **50**, 2389 (1989).

[51] W. Häckl, U. Seifert, and E. Sackmann, Journal de Physique II **7**, 1141 (1997).

[52] J. Pécréaux, H. G. Döbereiner, J. Prost, J. F. Joanny, and P. Bassereau, Eur. Phys. J. E **13**, 277 (2004).

[53] R. Rodríguez-García, I. López-Montero, M. Mell, G. Egea, N. S. Gov, and F. Monroy, Biophys. J. **108**, 2794 (2015).

[54] S. Ramaswamy, J. Toner, and J. Prost, Phys. Rev. Lett. **84**, 3494 (2000).

[55] N. Gov, Phys. Rev. Lett. **93**, 268104 (2004).

[56] A. E. Patteson, A. Vahabikashi, K. Pogoda, S. A. Adam, K. Mandal, M. Kittisopikul, S. Sivagurunathan, A. Goldman, R. D. Goldman, and P. A. Janmey, J. Cell Biol. **218**, 4079 (2019).

[57] J. F. Rupprecht, A. S. Vishen, G. V. Shivashankar, M. Rao, and J. Prost, Phys. Rev. Lett. **120**, 098001 (2018).

[58] K. Keren, Z. Pincus, G. M. Allen, E. L. Barnhart, G. Marriott, A. Mogilner, and J. A. Theriot, Nature **453**, 475 (2008).

[59] J. Y. Tinevez and et al., Proc. Natl. Acad. Sci. **106**, 18581 (2009).

[60] E. L. Barnhart, K. C. Lee, K. Keren, A. Mogilner, and J. A. Theriot, PLoS Biol **9**, e1001059 (2011).

[61] C. A. Wilson, M. A. Tsuchida, G. M. Allen, E. L. Barnhart, K. T. Applegate, P. T. Yam, L. Ji, K. Keren, G. Danuser, and J. A. Theriot, Nature **465**, 373 (2010).

[62] G. Koenderink and E. Paluch, Curr. Op. Cell Biol. **50**, 79 (2018).

[63] B. J. Belin, T. Lee, and R. D. Mullins, eLife **4**, e07735 (2015).

[64] Y. Wang, A. Sherrard, B. Zhao, M. Melak, J. Trautwein, E. M. Kleinschnitz, N. Tsopoulidis, O. T. Fackler, C. Schwan, and R. Grosse, Nat. Commun. **10**, 5271 (2019).

[65] N. Lamm, M. N. Read, M. Nobis, D. Van Ly, S. G. Page, V. P. Masamsetti, P. Timpson, M. Biro, and A. J. Cesare, Nat. Cell Biol. **22**, 1460 (2020).

[66] Y. Takahashi, S. Hiratsuka, N. Machida, D. Takahashi, J. Matsushita, P. Hozak, T. Misteli, K. Miyamoto, and M. Harata, Nucleus **11**, 250 (2020).

[67] A. D. Stephens and et al., Mol. Biol. Cell **29**, 220 (2018).

[68] A. D. Stephens, P. Z. Liu, V. Kandula, H. Chen, L. M. Almassalha, C. Herman, V. Backman, T. O'Halloran, S. A. Adam, R. D. Goldman, E. J. Banigan, and J. F. Marko, Mol. Biol. Cell **30**, 2320 (2019).